



OPEN

Cortical oscillations that underlie visual selective attention are abnormal in adolescents with cerebral palsy

Rashelle M. Hoffman^{1,2}, Christine M. Embury¹, Brandon J. Lew¹, Elizabeth Heinrichs-Graham¹, Tony W. Wilson¹ & Max J. Kurz¹✉

Adolescence is a critical period for the development and refinement of several higher-level cognitive functions, including visual selective attention. Clinically, it has been noted that adolescents with cerebral palsy (CP) may have deficits in selectively attending to objects within their visual field. This study aimed to evaluate the neural oscillatory activity in the ventral attention network while adolescents with CP performed a visual selective attention task. Adolescents with CP (N = 14; Age = 15.7 ± 4 years; MACS I–III; GMFCS I–IV) and neurotypical (NT) adolescents (N = 21; Age = 14.3 ± 2 years) performed the Eriksen flanker task while undergoing magnetoencephalographic (MEG) brain imaging. The participants reported the direction of a target arrow that was surrounded by congruent or incongruent flanking arrows. Compared with NT adolescents, adolescents with CP had slower responses and made more errors regarding the direction of the target arrow. The MEG results revealed that adolescents with CP had stronger alpha oscillations in the left insula when the flanking arrows were incongruent. Furthermore, participants that had more errors also tended to have stronger alpha oscillatory activity in this brain region. Altogether these results indicate that the aberrant activity seen in the left insula is associated with diminished visual selective attention function in adolescents with CP.

Cerebral palsy (CP) stems from a perinatal brain insult and is the most common pediatric motor disability, impacting 3.1 per 1000 live births in the United States^{1,2}. In addition to the motor impairments, some individuals with CP have visual attention deficits compared to their age matched peers³. Adolescence is a key developmental period for the refinement of several cognitive functions, including visual perception⁴. Such maturational changes in visual perceptual processes are paralleled by developmental shifts in the frontal lobes, a region strongly associated with attention and executive processes⁵. The current view is that the impairments in visual perception often seen in adolescents with CP may result from acuity, retinopathy of prematurity, and/or strabismus^{6,7}. Such visual deficits may disrupt the ability to selectively attend to a visual stimulus while performing goal-oriented motor behaviors. Although this is plausible, this conjecture has not been specifically tested.

The ability to focus on a target visual stimulus while disregarding distracting or unrelated stimuli is central to visual selective attention function^{8,9}. The classic Eriksen flanker task has been widely utilized to probe visual selective attention¹⁰. This task requires participants to focus on a target visual stimulus and disregard the surrounding “flanker” stimuli. The task includes trials with flanking stimuli that are identical to the target stimuli (e.g., arrows pointing the same direction; congruent trials) and trials where the flanking stimuli are the opposite of the target stimuli (e.g., arrows pointing in the opposite direction; incongruent trials). Behaviorally, this task elicits a robust difference commonly termed the “flanker effect,” whereby participants are less accurate and/or respond more slowly on incongruent compared to congruent trials, which is interpreted as an inability to fully suppress the interference caused by the distracting, incongruent flanking arrows^{11,12}. Magnetoencephalographic (MEG) brain imaging has indicated that there are changes in the strength of the theta (4–8 Hz) and alpha (8–12 Hz) cortical oscillations in the temporoparietal junction, the ventral frontal cortex, and the insula while performing this task^{11–16}. These neural generators comprise the ventral attention network, which is thought to

¹Institute for Human Neuroscience, Boys Town National Research Hospital, 14000 Boys Town Hospital Road, Boys Town, NE 68010, USA. ²Department of Physical Therapy, Munroe-Meyer Institute, University of Nebraska Medical Center, Omaha, NE, USA. ✉email: max.kurz@boystown.org

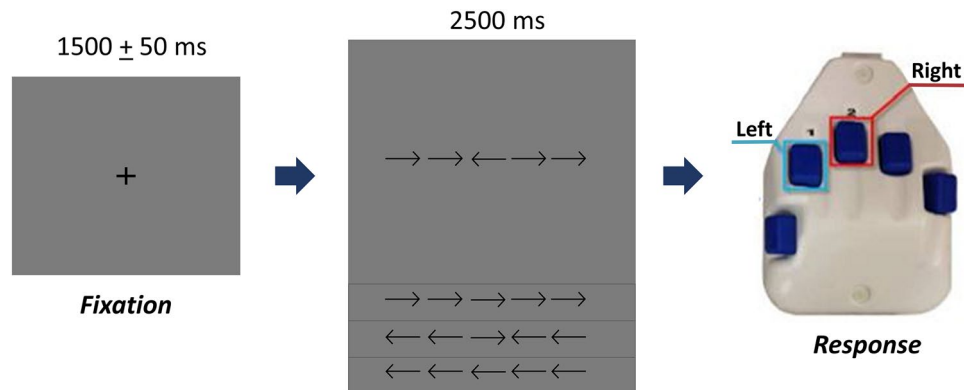


Figure 1. The Eriksen Flanker task paradigm. For each trial, the adolescents fixated on a crosshair for 1500 ± 50 ms, then a display with a series of five arrows appeared for 2500 ms. The adolescents responded with their right hand regarding the direction of the center arrow (left: 2nd digit, right: 3rd digit). In the congruent condition, the flanking arrows pointed in the same direction as the middle arrow, whereas in the incongruent condition the flanking arrows pointed in the opposite direction.

facilitate stimulus detection amidst distracting stimuli. Despite the growing recognition of the role of the ventral attention network, we have limited knowledge about the function of this network in individuals with CP.

This investigation used MEG brain imaging and advanced image reconstruction methods to evaluate cortical oscillations within the ventral attention network as adolescents with CP performed an arrow-based version of the flanker visual selective attention task. We hypothesized that (1) the visual attention-related cortical oscillations would be aberrant in adolescents with CP compared with neurotypical (NT) adolescents, and (2) that these atypical cortical oscillations would be tightly coupled with the speed and accuracy of their behavioral response on the direction of the target arrow.

Methods

Participants. NT adolescents and those with CP participated in this cross-sectional investigation. The adolescents with CP were referred from staff occupational and physical therapists at the Munroe-Meyer Institute who provide educational services. The adolescents with CP included in this study had primarily white matter injuries and no volume loss that would affect the integrity of the cortical surface. Adolescents were excluded from participating in this study if their cognitive function was too low to complete the Eriksen Flanker task, they had metal in their body that would preclude the use of MEG, or prior surgery and/or botulinum toxin injections in the past 6 months. Each adolescent and their parent/guardian provided written and informed assent/consent, respectively, to participate in the investigation. The protocol for this investigation was approved by University of Nebraska Medical Center's Institutional Review Board and in compliance with the Code of Ethics of the World Medical Association. Effectively, all of the methods used in this investigation were performed in accordance with the relevant guidelines and regulations.

Experimental design. Of note, the methodology employed in the current investigation is similar to what has been utilized in our prior experimental studies^{11,12,16–27}.

Neuromagnetic responses were sampled continuously at 1 kHz with an acquisition bandwidth of 0.1–330 Hz using a MEGIN MEG system (Helsinki, Finland). The participants completed an arrow-based version of the Eriksen flanker task¹⁰. Each trial began with a fixation cross that was presented for an interval of 1500 ± 50 ms. A row of five arrows was then presented for 2500 ms and the adolescents were instructed to respond as to the direction of the center target arrow with their second (left arrow) or third (right arrow) digit of the right hand using a custom 5-button pad (Fig. 1). Visual presentation consisted of either a series of flanking arrows that had directions that were congruent (i.e., same direction) or incongruent (i.e., opposite direction) with the middle target arrow. The task stimuli was projected onto a screen that was approximately one meter from the participant. A total of 200 trials were presented, making the overall MEG recording time about 14 min. Trials were equally split and pseudo-randomized between congruent and incongruent conditions, with left and right pointing arrows being equally represented in each condition. Only correct responses were included for further analysis.

MEG coregistration, MEG pre-processing and source imaging. Four coils were affixed to the participant's head and were used for continuous head localization. Prior to the experiment, the location of these coils, three fiducial points, and the scalp surface were digitized to determine their three-dimensional position (Fastrak 3SF0002, Polhemus Navigator Sciences, Colchester, VT, USA). The coil locations during the MEG acquisition and the scalp surface points were used to coregister the MEG data with the native space neuroanatomical MRI data.

Using the MaxFilter software (MEGIN), each MEG dataset was individually corrected for head motion that may have occurred during task performance and was subjected to noise reduction using the signal space

	Cerebral palsy (N = 14)	Neurotypical (N = 21)
Age (years)	15.7 ± 4.0	14.3 ± 2.0
Gender (male)	7	13
MACS		N/A
I	4	
II	7	
III	3	
Type of cerebral palsy		N/A
Diplegic	11	
Hemiplegic	3	

Table 1. Participant demographics. Participant demographics are displayed for the group with CP and the NT group. Abbreviations: manual ability classification system (MACS).

separation method with a temporal extension²⁸. Artifact rejection was based on a fixed threshold method, supplemented with visual inspection. The continuous magnetic time series was divided into epochs of 2000 ms in duration, with 0 ms defined as the stimulus onset and the baseline being – 450 to – 50 ms. Artifact-free epochs for each sensor were transformed into the time–frequency domain using complex demodulation and averaged over the respective trials. These sensor-level data were then normalized per time–frequency bin using the mean power for the specific frequency during the baseline (– 450 to – 50 ms). The specific time–frequency windows used for imaging were determined by statistical analysis of the sensor-level spectrograms across the entire array of gradiometers. The specific time–frequency windows used for imaging were determined by statistical analysis of the sensor-level spectrograms across the entire array of gradiometers. This involved performing 1000 cluster based permutation paired-sample t-tests to define time–frequency bins containing potentially significant oscillatory deviations^{29,30}. Note that the determination of the time–frequency windows to image was based on the spectrograms created from the entire group and both Flanker conditions. Additional information on our data processing pipeline is available in Weisman and Wilson³¹.

A beamforming algorithm was employed to calculate the source power across the entire brain volume³². The single images were derived from the cross spectral densities of all combinations of MEG sensors, and the solution of the forward problem for each location on a grid specified by input voxel space. Following convention, the source power in these images was normalized per subject using a separately averaged pre-stimulus noise period of equal duration and bandwidth^{33–35}. Thus, the normalized power per voxel (pseudo-t) was computed over the entire brain volume per adolescent at 4.0 × 4.0 × 4.0 mm resolution. Each adolescent's functional images, which were co-registered to their structural T1-weighted MRI prior to beamforming, were transformed into standardized space using the transform previously applied to the structural MRI volume and spatially resampled. MEG pre-processing and imaging used the BESA software (BESA v6.0; Grafelfing, Germany). A whole-brain repeated-measures ANOVA (congruent/incongruent × group) was subsequently completed for each time–frequency window of interest to determine locations of significant voxel clusters.

Motor behavioral data. The output of the button pad was simultaneously collected at 1 kHz along with the MEG data. The time the participant took to decide the direction of the target arrow (i.e., reaction time) was calculated based on the time from when the arrow array was presented to when the button was pressed. Accuracy was defined as the percentage of correct responses divided by the total number of trials. Separate repeated-measures ANOVAs (congruent/incongruent × group) were used to evaluate differences in the respective behavioral outcome measures. Lastly, Spearman rho rank-order correlations were used to determine potential relationships between behavioral and neuronal outcome metrics.

Results

Fourteen adolescents with CP (Age = 15.7 ± 4.0 years; MACS levels I–III) and twenty-one NT adolescents (Age = 14.3 ± 2.0 years) fit the inclusion criteria and participated in this investigation. Further information on the respective participants can be found in Table 1.

Behavioral results. There was a significant main effect of condition (congruent vs. incongruent) for the reaction time, which is consistent with the well-established “flanker effect” indicating that the adolescents took longer to respond during the incongruent compared to the congruent condition, likely due to the visually distracting flanking arrows (congruent = 785.3 ± 38.6 ms, incongruent = 849.7 ± 40.5 ms; $P < 0.001$). Additionally, there was a main effect of group, signifying that the adolescents with CP had slower reaction times relative to the NT adolescents across both conditions (CP = 1054.2 ± 78.4 ms, NT = 692.3 ± 23.9 ms; $P < 0.001$; Fig. 2a.). The group-by-condition interaction for reaction time was not significant ($P = 0.4$).

A Shapiro–Wilk test of the accuracy data indicated the sample data was not normally distributed ($P < 0.001$). Therefore, the accuracy data was log-transformed for statistical analysis. We found a main effect of condition ($P = 0.006$), indicating that adolescents were less accurate during the incongruent condition (congruent = 96.7 ± 1.1%; incongruent = 93.5 ± 2.2%; Fig. 2b). Additionally, there was a main effect of group ($P = 0.004$), indicating that the adolescents with CP were less accurate overall relative to the NT adolescents (CP = 87.5 ± 3.9%;

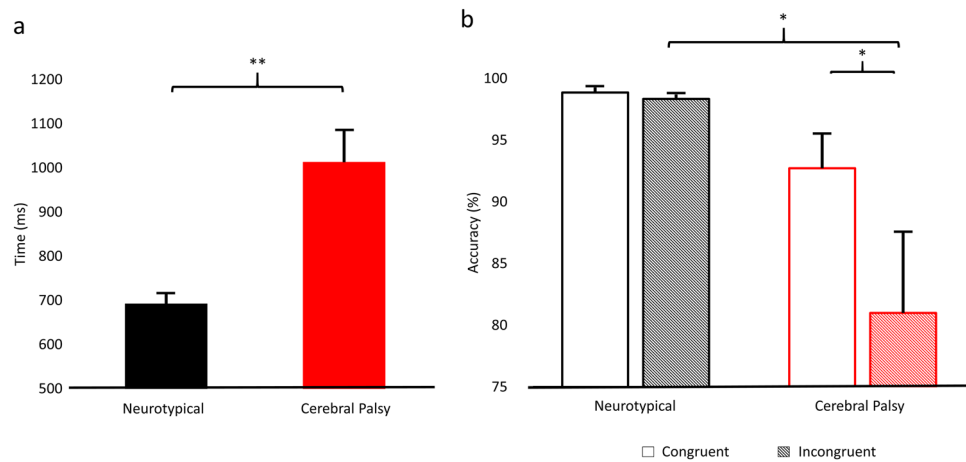


Figure 2. Reaction time and accuracy for neurotypical adolescents and adolescents with cerebral palsy. Repeated-measures analysis of variance of reaction time (a) and accuracy (b). Reaction time results revealed significant main effects of condition and group ($P < 0.001$), but no interaction effect ($P = 0.4$). The main effect of condition indicates slower reaction times for the incongruent condition compared to the congruent condition, while the main effect of group indicates that individuals with cerebral palsy responded slower than the neurotypical group. (a) Depicts the group effect ($P < 0.001$). Accuracy results revealed main effects of condition ($P = 0.006$), group ($P = 0.004$), and an interaction effect ($P = 0.009$). The main effect of condition reflected less accuracy for the incongruent compared to the congruent condition, while the main effect of group indicated that those with cerebral palsy were less accurate than the neurotypical adolescents. Post-hoc significance levels are displayed above the data, with error bars indicating the SEM. * $P < 0.05$, ** $P < 0.001$.

NT = $99.9 \pm 0.2\%$). Lastly, there was a significant group-by-condition interaction ($P = 0.009$). Post-hoc analysis showed that the adolescents with CP were significantly less accurate for the incongruent condition (incongruent = $81.0\% \pm 6.5\%$; congruent = $92.7\% \pm 2.8\%$; $P = 0.037$), while this effect was trending in the NT adolescents (incongruent = $98.3\% \pm 0.3\%$; congruent = $98.9\% \pm 0.4\%$; $P = 0.099$). When comparing within each condition, the adolescents with CP were significantly less accurate than the NT adolescents in the incongruent condition (CP = $81.0 \pm 6.5\%$; NT = $98.3 \pm 0.3\%$; $P = 0.027$) and marginally so for the congruent condition (CP = $92.7 \pm 2.8\%$; NT = $98.9 \pm 0.4\%$; $P = 0.055$).

Sensor level results. Time frequency analyses were conducted across all participants and gradiometer sensors and these were examined statistically to identify the time–frequency windows of interest for follow-up beamforming analysis. These analyses revealed significant alpha (8–14 Hz) event-related desynchronization (ERD) and theta (4–8 Hz) event-related synchronization (ERS) responses concentrated in a large number of sensors within the frontal cortices and stretching towards the parietal lobule ($P < 0.0001$, corrected). Desynchronizations indicate a decrease in power while synchronizations indicate an increase in power compared to the baseline window (–450 to –50 ms). For illustrative purposes, we show group-averaged time frequency spectrograms collapsed across groups and conditions in Fig. 3. The sensor-level statistical analyses indicated that there was a prominent alpha ERD about 250 ms after stimulus onset that extended until 650 ms (i.e., 250–650 ms; Fig. 3a). Additionally, there was a theta ERS that began about 200 ms after stimulus onset (0 ms) and was sustained until 600 ms (i.e., 200–600 ms; Fig. 3b).

MEG imaging of cortical oscillations. Beamforming was used to image the significant alpha (8–14 Hz) response identified in the sensor level spectrograms during the 250–650 ms time window with a baseline of –450 to –50 ms. A whole-brain repeated-measures ANOVA (condition \times group) was conducted with an α level of 0.001 and a cluster threshold of 200 voxels. This analysis revealed a significant condition effect in the right inferior frontal gyrus, indicating that there was less of a reduction in the strength of the alpha oscillations during the incongruent condition. Furthermore, there was an interaction in the left insula (Fig. 3c). Post-hoc analyses performed for the interaction showed that there was a stronger alpha ERD in the left insula for the adolescents with CP ($P = 0.004$) and NT adolescents ($P = 0.02$) during the incongruent compared to the congruent condition, and that the adolescents with CP had a stronger alpha ERD compared to NT adolescents in the incongruent ($P = 0.02$), but not the congruent condition ($P = 0.7$) in this cortical region.

Beamforming was also used to image the significant theta (4–8 Hz) response using the identified 200–600 ms time window and a baseline period of –450 to –50 ms. These data were also examined using whole-brain repeated-measures ANOVA (condition \times group) approach with an α level of 0.001 and a cluster threshold of 200 voxels. We found a significant condition effect in the right dorsal lateral prefrontal cortices, left premotor cortices, and anterior cingulate. This indicated that there was a greater increase in the strength of the theta oscillations during the incongruent condition for the respective areas. There also was an interaction in the anterior right middle frontal gyrus (Fig. 3d). Post-hoc statistical analyses revealed that both the adolescents with CP

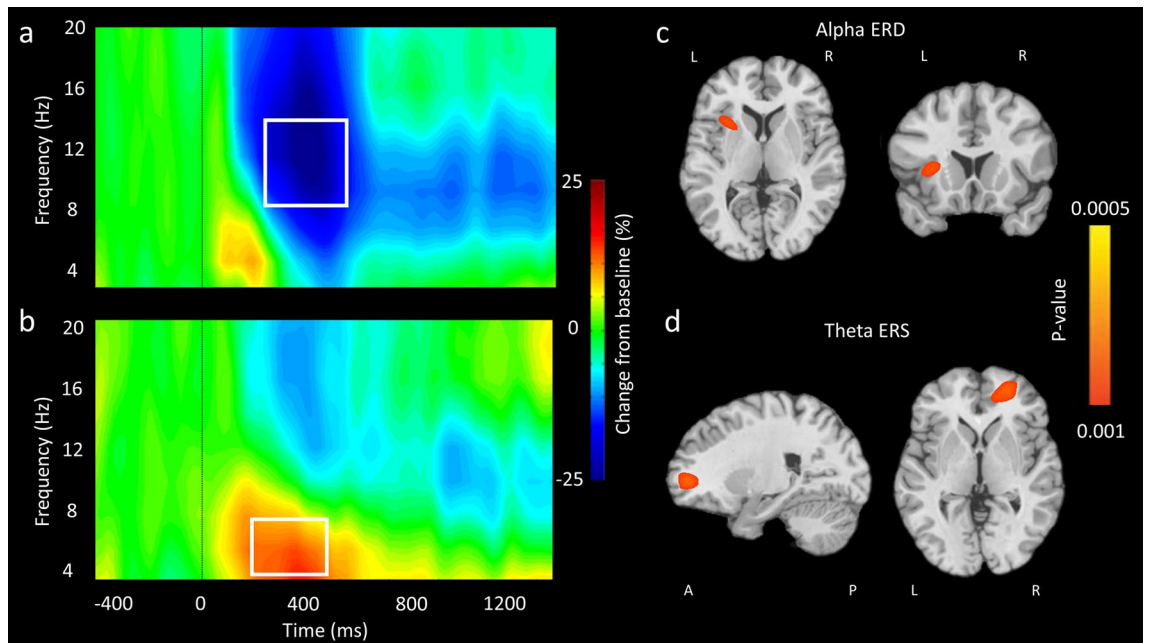


Figure 3. MEG sensor-level activity and whole brain repeated-measures ANOVA results for alpha ERD and theta ERS responses. MEG sensor-level grand-averaged spectrograms for the alpha ERD response in a sensor located over the parietal cortex (a), and the theta ERS response in a sensor located over the frontal cortex (b). In each, time (ms) is represented on the x-axis with 0 ms indicating stimulus onset (i.e., when arrows appeared). Relative spectral power is expressed as a percentage difference from baseline, with the color legend shown to the right of the spectrograms. As shown, there was a prominent alpha ERD (8–14 Hz) that began about 250 ms after stimulus onset and lasted until 650 ms. Additionally, there was a theta ERS (4–8 Hz) that began 200 ms after stimulus onset and was sustained until 600 ms. Whole-brain repeated-measures ANOVAs (condition \times group) revealed an interaction for the alpha oscillations (8–14 Hz) in the left insula (c), while the same analysis for theta oscillations (4–8 Hz) showed an effect in the right middle frontal gyrus (d). All source images were created using NeuroElf V1.1 (<https://neuroelf.net/>).

($P=0.04$) and NT adolescents ($P=0.008$) had significantly stronger theta ERS for the incongruent compared to the congruent condition in this region. No significant differences were found between groups for congruent or incongruent conditions ($P>0.05$).

Neuro-behavioral correlations. There was a significant rank-order relationship between the strength of the alpha ERD in the left insula and accuracy ($\rho=0.550$, $P=0.001$). This finding was for the incongruent condition only when collapsed across groups. Additionally, there was a significant rank-order relationship between the strength of the alpha ERD in the left insula and accuracy for the incongruent condition in the CP group only ($\rho=0.670$, $P=0.009$; Fig. 4). Both correlations imply that the participants with a stronger alpha ERD tended to be less accurate in identifying the direction of the target arrow, which is consistent with our ANOVA results (see above). No other correlations between behavioral and neuronal outcomes measures were significant ($P>0.05$).

Discussion

Overall our experimental results for the NT adolescents and those with CP were well aligned with the prior MEG experimental outcomes using this task, which have shown there is an alpha ERD in the left insula and a theta ERS in the right middle frontal gyrus during task performance^{11–16}. Furthermore, in line with previous studies, the neural oscillations for the incongruent condition were stronger than those detected in the congruent condition^{16,17,36}. When we compared the strength of these neural oscillations between the respective groups, we identified that the adolescents with CP had a stronger alpha ERD than the NT adolescents in the left insula during the incongruent condition. Previous studies have suggested that a stronger alpha ERD reflects greater attentional demands created by the distracting incongruent arrows^{11,12,16}. Based on this notion, we suspect that the stronger alpha ERD seen in the adolescents with CP might indicate that they utilize even greater cortical resources in attending to the visual stimulus amidst the distracting stimuli.

Compared with the NT adolescents, the adolescents with CP were slower to respond and made more errors in their perception of the target arrow's direction. These behavioral results further support the notion that adolescents with CP have greater difficulty performing tasks that require selective visual attention. Our correlational results also indicated that participants that had greater behavioral errors also tended to have a stronger alpha ERD. Altogether these results further fuel the impression that the stronger alpha ERD observed in the adolescents with CP might represent greater difficulty in focusing on the target stimulus in the context of the distracting stimuli. We propose that the relationship observed between the alpha ERD and performance reflects that participants with CP who are poorer performers activate this region more strongly, but that ultimately this

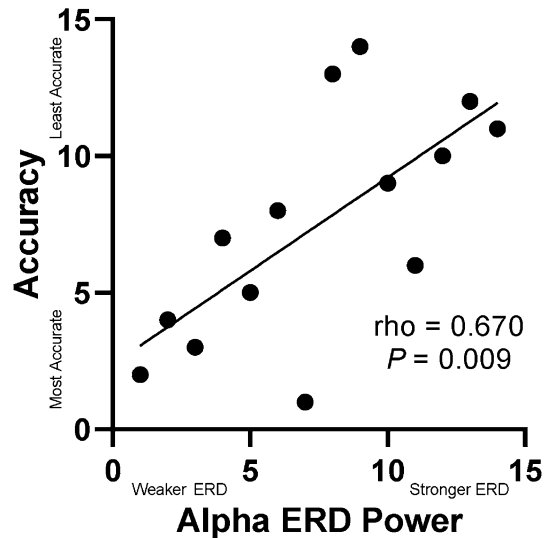


Figure 4. Rank-order correlation analysis between accuracy and alpha ERD Power. The alpha ERD peak voxel was identified in the left insula interaction effect map for the incongruent condition in the CP group only. Rank-order of the alpha ERD is shown on the x-axis, while the rank-order of accuracy is shown on the y-axis. As shown, there was a significant positive correlation between the strength of the change in the alpha ERD and the participant's accuracy ($\rho = 0.670$; $P = 0.009$). This correlation implies that adolescents with CP that had stronger alpha oscillations in the left insula also tended to make more errors in their perception of the target arrow's direction. ERD event-related desynchronization.

stronger activation is not enough to boost performance to normal levels. However, future studies are warranted as there could also be downstream effects that modulate performance, and/or aberrant activity in upstream brain regions that may be providing inferior information to this circuit necessitating that it work harder during task performance.

We recognize that there are limitations in our experimental approach. For one, the sample size for the adolescents with CP was relatively small and may not reflect the wide variety of neurologic impairments seen in individuals with CP. Second, there is growing appreciation that the timing of the perinatal insult may at least partially account for the nature of the structural brain differences (i.e., malformation, white matter injury) and possibly the variety of sensorimotor presentation seen in individuals with CP^{37,38}. It is also possible that the type of perinatal brain insult may influence the activity of other nodes within the ventral attention network. Unfortunately, we cannot address this proposition since the participants in our study had white matter injuries. Furthermore, we are cautionary with this conjecture because the relationship between the type of brain insult and the resultant alterations in cortical activity is not well established. In summary, this study has provided new insight on the neural and behavioral aberrations that underlie selective attention deficits in adolescents with CP, but additional work in this area is critical.

Data availability

Data generated during the current study are available upon reasonable request and IRB approval.

Received: 3 December 2020; Accepted: 4 February 2021

Published online: 25 February 2021

References

- Rosenbaum, P. *et al.* A report: the definition and classification of cerebral palsy April 2006. *Dev. Med. Child Neurol. Suppl.* **109**, 8–14 (2007).
- Christensen, D. *et al.* Prevalence of cerebral palsy, co-occurring autism spectrum disorders, and motor functioning—autism and developmental disabilities monitoring network, USA, 2008. *Dev. Med. Child Neurol.* **56**, 59–65. <https://doi.org/10.1111/dmcn.12268> (2014).
- Botcher, L., Flachs, E. M. & Uldall, P. Attentional and executive impairments in children with spastic cerebral palsy. *Dev. Med. Child Neurol.* **52**, e42–e47. <https://doi.org/10.1111/j.1469-8749.2009.03533.x> (2010).
- Alvarez, J. A. & Emory, E. Executive function and the frontal lobes: a meta-analytic review. *Neuropsychol. Rev.* **16**, 17–42. <https://doi.org/10.1007/s11065-006-9002-x> (2006).
- Rubia, K. *et al.* Functional frontalisation with age: mapping neurodevelopmental trajectories with fMRI. *Neurosci. Biobehav. Rev.* **24**, 13–19. [https://doi.org/10.1016/s0149-7634\(99\)00055-x](https://doi.org/10.1016/s0149-7634(99)00055-x) (2000).
- Ego, A. *et al.* Visual-perceptual impairment in children with cerebral palsy: a systematic review. *Dev. Med. Child Neurol.* **57**(Suppl 2), 46–51. <https://doi.org/10.1111/dmcn.12687> (2015).
- Guzzetta, A., Mercuri, E. & Cioni, G. Visual disorders in children with brain lesions: 2. Visual impairment associated with cerebral palsy. *Eur. J. Paediatr. Neurol.* **5**, 115–119. <https://doi.org/10.1053/ejpn.2001.0481> (2001).
- Carrasco, M. Visual attention: the past 25 years. *Vis. Res.* **51**, 1484–1525. <https://doi.org/10.1016/j.visres.2011.04.012> (2011).
- Driver, J. A selective review of selective attention research from the past century. *Br. J. Psychol.* **92** Part 1, 53–78 (2001).

10. Eriksen, B. A. & Eriksen, C. W. Effects of noise letters upon the identification of a target letter in a nonsearch task. *Percept. Psychophys.* **16**, 143–149. <https://doi.org/10.3758/bf03203267> (1974).
11. McDermott, T. J., Wiesman, A. I., Proskovec, A. L., Heinrichs-Graham, E. & Wilson, T. W. Spatiotemporal oscillatory dynamics of visual selective attention during a flanker task. *Neuroimage* **156**, 277–285. <https://doi.org/10.1016/j.neuroimage.2017.05.014> (2017).
12. McDermott, T. J. *et al.* tDCS modulates behavioral performance and the neural oscillatory dynamics serving visual selective attention. *Hum. Brain Mapp.* <https://doi.org/10.1002/hbm.24405> (2019).
13. Corbetta, M. & Shulman, G. L. Control of goal-directed and stimulus-driven attention in the brain. *Nat. Rev. Neurosci.* **3**, 201–215. <https://doi.org/10.1038/nrn755> (2002).
14. Corbetta, M., Patel, G. & Shulman, G. L. The reorienting system of the human brain: from environment to theory of mind. *Neuron* **58**, 306–324. <https://doi.org/10.1016/j.neuron.2008.04.017> (2008).
15. Webb, T. W., Igelstrom, K. M., Schurger, A. & Graziano, M. S. Cortical networks involved in visual awareness independent of visual attention. *Proc. Natl. Acad. Sci. U. S. A.* **113**, 13923–13928. <https://doi.org/10.1073/pnas.1611505113> (2016).
16. Lew, B. J. *et al.* Neural dynamics of selective attention deficits in HIV-associated neurocognitive disorder. *Neurology* **91**, e1860–e1869. <https://doi.org/10.1212/wnl.0000000000006504> (2018).
17. Embury, C. M. *et al.* The impact of type 1 diabetes on neural activity serving attention. *Hum. Brain Mapp.* **40**, 1093–1100. <https://doi.org/10.1002/hbm.24431> (2019).
18. Gehring, J. E., Arpin, D. J., Heinrichs-Graham, E., Wilson, T. W. & Kurz, M. J. Neurophysiological changes in the visuomotor network after practicing a motor task. *J. Neurophysiol.* **120**, 239–249. <https://doi.org/10.1152/jn.00020.2018> (2018).
19. Trevarrow, M. P. *et al.* The developmental trajectory of sensorimotor cortical oscillations. *NeuroImage* **184**, 455–461. <https://doi.org/10.1016/j.neuroimage.2018.09.018> (2019).
20. Arpin, D. J. *et al.* Altered sensorimotor cortical oscillations in individuals with multiple sclerosis suggests a faulty internal model. *Hum. Brain Mapp.* **38**, 4009–4018. <https://doi.org/10.1002/hbm.23644> (2017).
21. Kurz, M. J., Proskovec, A. L., Gehring, J. E., Heinrichs-Graham, E. & Wilson, T. W. Children with cerebral palsy have altered oscillatory activity in the motor and visual cortices during a knee motor task. *Neuroimage Clin.* **15**, 298–305. <https://doi.org/10.1016/j.nicl.2017.05.008> (2017).
22. Spooner, R. K. *et al.* Aberrant oscillatory dynamics during somatosensory processing in HIV-infected adults. *NeuroImage Clin.* **20**, 85–91. <https://doi.org/10.1016/j.nicl.2018.07.009> (2018).
23. Hoffman, R. M., Wilson, T. W. & Kurz, M. J. Hand motor actions of children with cerebral palsy are associated with abnormal sensorimotor cortical oscillations. *Neurorehabil. Neural Repair* **33**, 1018–1028. <https://doi.org/10.1177/1545968319883880> (2019).
24. Gehring, J. E. *et al.* The strength of the movement-related somatosensory cortical oscillations differ between adolescents and adults. *Sci. Rep.* **9**, 18520–18520. <https://doi.org/10.1038/s41598-019-55004-1> (2019).
25. Wilson, T. W., Heinrichs-Graham, E., Proskovec, A. L. & McDermott, T. J. Neuroimaging with magnetoencephalography: a dynamic view of brain pathophysiology. *Transl. Res.* **175**, 17–36. <https://doi.org/10.1016/j.trsl.2016.01.007> (2016).
26. Lew, B. J. *et al.* Interactive effects of HIV and ageing on neural oscillations: independence from neuropsychological performance. *Brain Commun.* **2**, fcaa015. <https://doi.org/10.1093/braincomms/fcaa015> (2020).
27. Wiesman, A. I. *et al.* Epigenetic markers of aging predict the neural oscillations serving selective attention. *Cereb. Cortex* **30**, 1234–1243. <https://doi.org/10.1093/cercor/bhz162> (2020).
28. Taulu, S. & Simola, J. Spatiotemporal signal space separation method for rejecting nearby interference in MEG measurements. *Phys. Med. Biol.* **51**, 1759–1768. <https://doi.org/10.1088/0031-9155/51/7/008> (2006).
29. Ernst, M. D. Permutation methods: a basis for exact inference. *Stat. Sci.* **19**, 676–685 (2004).
30. Maris, E. & Oostenveld, R. Nonparametric statistical testing of EEG- and MEG-data. *J. Neurosci. Methods* **164**, 177–190 (2007).
31. Wiesman, A. I. & Wilson, T. W. Attention modulates the gating of primary somatosensory oscillations. *Neuroimage* **211**, 116610. <https://doi.org/10.1016/j.neuroimage.2020.116610> (2020).
32. Gross, J. *et al.* Dynamic imaging of coherent sources: studying neural interactions in the human brain. *Proc. Natl. Acad. Sci. U. S. A.* **98**, 694–699. <https://doi.org/10.1073/pnas.98.2.694> (2001).
33. Hillebrand, A., Singh, K. D., Holliday, I. E., Furlong, P. L. & Barnes, G. R. A new approach to neuroimaging with magnetoencephalography. *Hum. Brain Mapp.* **25**, 199–211. <https://doi.org/10.1002/hbm.20102> (2005).
34. Hillebrand, A. & Barnes, G. R. Beamformer analysis of MEG data. *Int. Rev. Neurobiol.* **68**, 149–171. [https://doi.org/10.1016/s0074-7742\(05\)68006-3](https://doi.org/10.1016/s0074-7742(05)68006-3) (2005).
35. Van Veen, B. D., van Drongelen, W., Yuchtman, M. & Suzuki, A. Localization of brain electrical activity via linearly constrained minimum variance spatial filtering. *IEEE Trans. Biomed. Eng.* **44**, 867–880. <https://doi.org/10.1109/10.623056> (1997).
36. Beaton, L. E., Azma, S. & Marinkovic, K. When the brain changes its mind: oscillatory dynamics of conflict processing and response switching in a flanker task during alcohol challenge. *PLoS ONE* **13**, e0191200. <https://doi.org/10.1371/journal.pone.0191200> (2018).
37. Himmelmann, K. & Uvebrant, P. Function and neuroimaging in cerebral palsy: a population-based study. *Dev. Med. Child Neurol.* **53**, 516–521. <https://doi.org/10.1111/j.1469-8749.2011.03932.x> (2011).
38. Himmelmann, K. *et al.* MRI classification system (MRICS) for children with cerebral palsy: development, reliability, and recommendations. *Dev. Med. Child Neurol.* **59**, 57–64. <https://doi.org/10.1111/dmcn.13166> (2017).

Acknowledgements

This work was partially supported by Grants from the National Institutes of Health (R01-HD086245; R01-HD101833), and a Promotion of Doctoral Studies I Scholarship from the Foundation for Physical Therapy Research.

Author contributions

R.H. participated in the data collections, analyzed/processed the collected data, and drafted/edited the manuscript. C.E. and B.L. analyzed/processed the collected data. M.K., T.W., and E.H.G. oversaw the study, developed the study concept/design, participated in the data collections, assisted with interpretation of the data, and edited the manuscript. The authors declare no competing interests.

Competing interests

The authors declare no competing interests.

Additional information

Correspondence and requests for materials should be addressed to M.J.K.

Reprints and permissions information is available at www.nature.com/reprints.

Publisher's note Springer Nature remains neutral with regard to jurisdictional claims in published maps and institutional affiliations.



Open Access This article is licensed under a Creative Commons Attribution 4.0 International License, which permits use, sharing, adaptation, distribution and reproduction in any medium or format, as long as you give appropriate credit to the original author(s) and the source, provide a link to the Creative Commons licence, and indicate if changes were made. The images or other third party material in this article are included in the article's Creative Commons licence, unless indicated otherwise in a credit line to the material. If material is not included in the article's Creative Commons licence and your intended use is not permitted by statutory regulation or exceeds the permitted use, you will need to obtain permission directly from the copyright holder. To view a copy of this licence, visit <http://creativecommons.org/licenses/by/4.0/>.

© The Author(s) 2021